SIMULATION OF WRINKLING PATTERNS IN WEBS

DUE TO NON-UNIFORM TRANSPORT CONDITIONS

by

Richard C. Benson, Han Chieh Chiu, John LaFleche, and Kenneth D. Stack

University of Rochester
Rochester, New York

INTRODUCTION

It is often observed that flexible membranes are prone to wrinkling when passed through a roller "nip", when transported over a guide, or when wound onto a roll. This is due to an unfortunate design incompatibility between the web's inability to withstand compressive stress, and the sensitivity and variability that exists in many transport devices.

Figure 1 illustrates a problem familiar in web transport. Nonuniform conditions along the length of the nip cause variability in the transport speed of the web. This will cause a gradual build-up of loading on the web until finally the imbalance is relieved. For thick webs, the imbalance may be relieved through a complicated stick-slip behavior in the nip itself. For thinner webs, the imbalance may cause buckling. Buckling, or wrinkling, is highly undesired as the wrinkle will often be drawn into the nip, and then creased and made permanent. Figure 1 shows two commonly observed wrinkling patterns colloquially called "rivers" and "lakes". Figure 2 shows three photographs of a web with dimensions 148 mm x 114 mm x 6 μm (5.8 in x 4.5 in x 0.25 mils). From top to bottom, the three wrinkling patterns are of the "rivers", "lakes", and shear-induced type.

It is the goal of this paper to examine a very thin web under different edge displacement conditions, and to assess the consequences on wrinkling. Three of the edge loading patterns will be chosen for their basic nature. Two other test cases will be based on nip transport conditions predicted in a companion paper in this conference by Diehl, Stack and Benson [22]. A geometry exhibiting shear wrinkles will be used in three final cases to compare different modelling approaches.

The basic tool for our analysis is "tension field" theory which has been developed over the past 60 years to analyze a number of flexible structures that can support

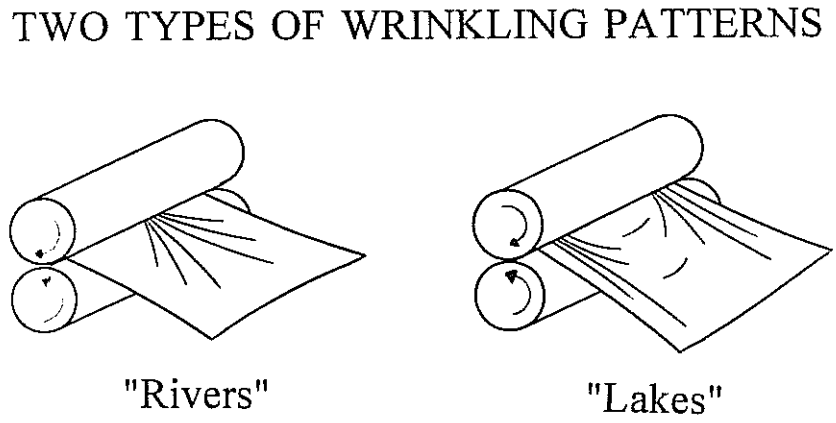

Figure 1: "Rivers" and "Lakes"

tension, but have virtually no ability to withstand compression. Application areas include airplane wing coverings, human skin, cloth, paper sheets, and polyethylene terephthalate (PET) webs. References [1-13,16-22] provide a sampling of the work that has been done in the past. The details of "tension field" theory, and more about individual references will be discussed in the next section.

WRINKLING ANALYSIS

The motivation for wrinkling analysis is to be able to analyze the load-bearing capability of exceedingly flexible membranes that may be locally buckled. To numerically calculate the out-of-plane deformation associated with buckling becomes increasingly more difficult as the membrane gets thinner, thus an alternative approach using only an in-plane description becomes desirable. Three different "tension field" theories have been developed, and are summarized below. Each theory shares the feature that only tensile stress is allowed to develop in the membrane. Compressive stresses are not allowed.

Generator Theory: This approach was developed by Kondo [3] and Mansfield [4,5,6] who observed that, for certain loading conditions, the wrinkles must be straight lines, and that they must not intersect within the borders of the membrane as stress singularities would occur. From this observation, it can be proved that each wrinkle line, or "generator" will touch tangent to a common curve called the "edge of regression". The mathematical task, then, is to find the edge of regression. (An analog of this same approach, incidentally, can also been used to model the large bending and twisting of inextensible sheets, like paper. See Darmon and Benson

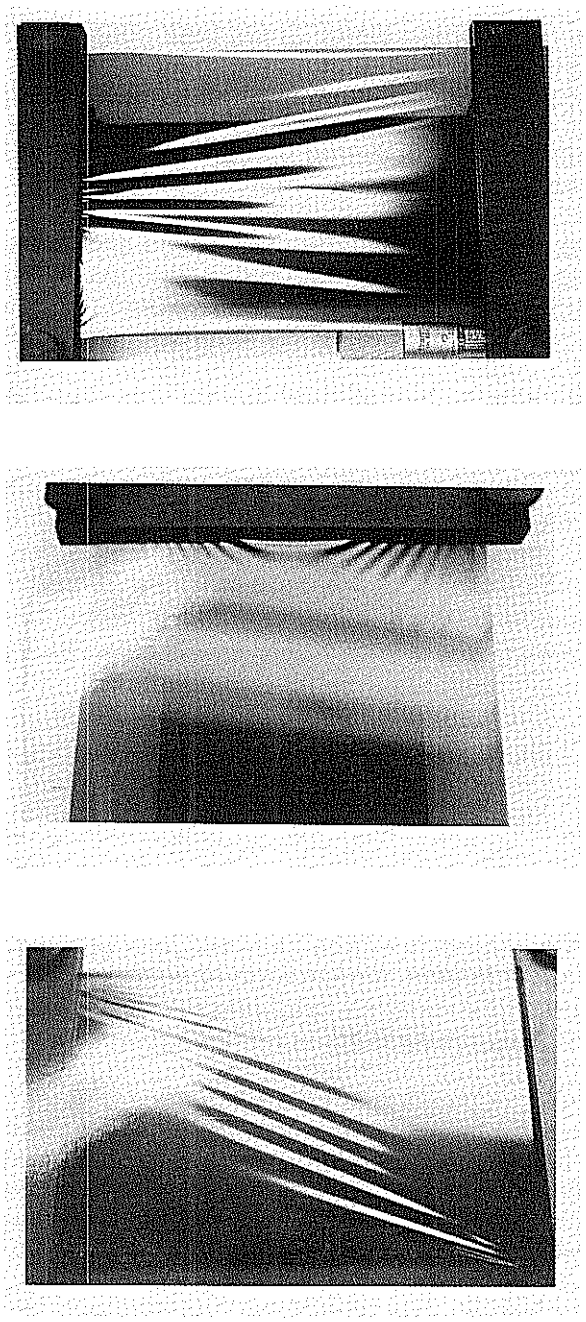

Figure 2: Photographs of Wrinkles
"Rivers" (top), "Lakes" (middle), Shear (bottom)

[14,15]).

The advantage of the "generator theory" is that large, nonlinear displacements can be treated. The mathematical treatment is very elegant and powerful. A significant disadvantage of the approach is that inhomogeneities within the membrane, or around the edges, cannot be treated. Thus, the approach can not be used, for example, for loads arising from thermal stresses, or from non-rigid-body displacement along an edge.

Method of False Material Constants: The earliest approach to wrinkling theory was developed by Wagner [1], and further developed by Reissner [2], and Miller and Hedgepeth [12,13]. The application areas included airplane wing covers, and human skin. A typical isotropic, planar stress-strain relationship is as follows:

$$\sigma_x = [E/(1-\nu^2)](\varepsilon_x + \nu\,\varepsilon_y), \quad \sigma_y = [E/(1-\nu^2)](\varepsilon_y + \nu\,\varepsilon_x), \quad \sigma_{xy} = [E/(1+\nu)]\varepsilon_{xy}. \quad (1)$$

Here, σ denotes stress, ε denotes strain, x and y are coordinate directions, E is Young's modulus, and ν is Poisson's ratio. The conventional principal stress calculation is to find a coordinate rotation by angle α, for which the shear stress vanishes, $\sigma_{xy} = 0$. Suppose, in the new principal coordinates, that this produces a tensile stress in the x direction, $\sigma_x > 0$, and a compressive stress in the y direction, $\sigma_y < 0$. If one ignored the fact that Poisson's ratio is a material *constant*, then ν could be artificially adjusted to drive the compressive stress back to zero, as follows:

$$\nu = -\varepsilon_y/\varepsilon_x. \quad (2)$$

Substituting this back into the stress-strain equations gives the desired result after wrinkling:

$$\sigma_x = E\,\varepsilon_x, \quad \sigma_y = 0, \quad \sigma_{xy} = 0 \quad (3)$$

Having changed σ_y, the equilibrium of the membrane has been disturbed, so it will also be necessary to recompute load balances, and recompute the angle, α, of the principal coordinates. In short, the two stress requirements, $\sigma_{xy} = 0$ and $\sigma_y = 0$, provide two equations for iteratively calculating the rotation angle to the coordinates of principal stresses, α, and the fictitious Poisson's ratio,ν.

The advantage of this approach is that it can be applied to general loading patterns, and can be utilized in a finite element model. The principal disadvantage is the need to treat material constants as adjustable parameters, and the resulting condition that the membrane must be characterized as an anisotropic, inhomogeneous, elastic material. The false material constants of the membrane will change whenever the applied loads change.

Wrinkle Strain Method: This concept was first introduced by Wu [7,8,10], and has been extended by Zak [9,11], Pipkin [16], Roddemann [17,18], and Steigman [19,20]. In the wrinkle strain method it is assumed that out-of-plane deflection relieves compressive stress across a wrinkle, and that there is an associated strain associated with this deflection. Consider, again, the stress/strain equations of (1). This time to drive σ_y to zero we adjust the *strain* in that direction:

$$\varepsilon_y = -\nu\,\varepsilon_x \qquad (4)$$

This also results in the desired form of equation (3). Note that E and ν are not altered. As with the method of false material constants, the wrinkle strain method couples two conditions, $\sigma_{xy} = 0$ and $\sigma_y = 0$, with two unknowns, α and ε_y.

The wrinkle strain method possesses several advantages. It allows for general loading. It may be utilized in a finite element model. It leaves material constants unaltered. And, it introduces a new strain measure that corresponds to out-of-plane displacement of the membrane. The principal drawback, which is shared by all three methods, is that without consideration of bending rigidity, no estimate can be made of the *wavelength* of the wrinkles.

Because of these perceived advantages, the wrinkle strain method is the approach being used by researchers at the University of Rochester, Mechanics of Flexible Structures Project. A Finite Element model with Wrinkling Analysis (FEWA) has been developed, and is used to make calculations in this paper. The finite element model was first developed by Roddemann et al. [17,18]. Further details, including an extension to thermal loading may be found in Chiu et al. [22]. The flowchart of the FEWA program is as follows:

1. Solve for in-plane deformation using conventional plane-stress methods.
2. Determine principal stresses.
3. Assess the character of each element:

   Taut, if both principal stresses are positive.
   Wrinkled, if one stress is positive and the other is negative.
4. Create element stiffness matrices, K:

   If taut, then K is unchanged.
   If wrinkled, then K is modified using the wrinkle strain method.
5. Assemble all element stiffness matrices into a global stiffness matrix.
6. Compute deflections using the modified global stiffness matrix.
7. Compute the total strain energy. Return to step 2 if not converged.

Table 1: FEWA Flowchart

This general approach is quite conventional in finite element analysis, except for steps 3 and 4. The fact that elements may be changing between taut and wrinkled characterizations makes the process nonlinear, and requires iteration to reach a final solution.

RESULTS

We have applied the FEWA code to a variety of boundary conditions to better understand the conditions that may lead to wrinkle formation. Figure 3 shows a finite element grid that is fixed at its left edge, and displaced rightward at its right edge. The top and bottom edges are stress free. There are 19x15 equally spaced nodes in the web. The geometry is scaled so that the short axis is 0.773 times the long axis. Displacements on the right edge will be given in parts-per-thousand of the length of the long edge. This geometry is motivated by the following physical

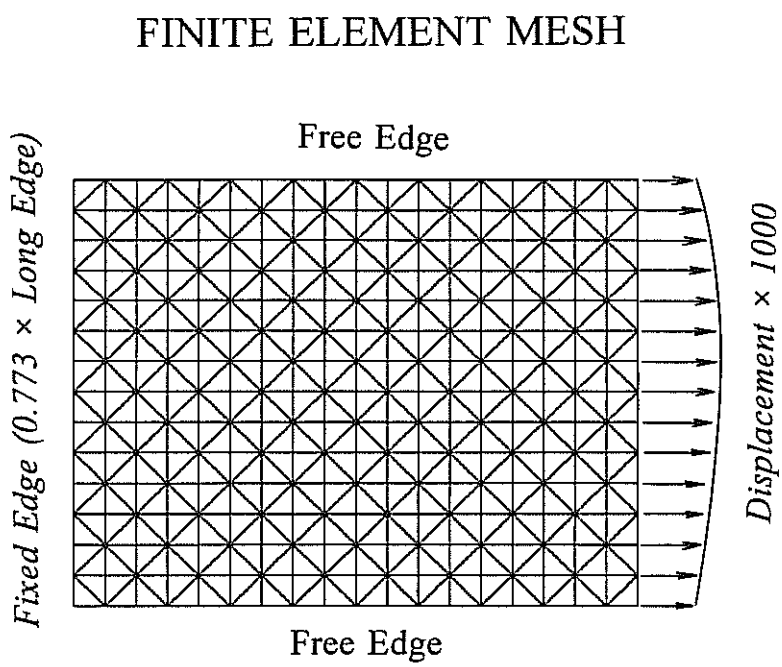

Figure 3: Finite Element Mesh

system of interest to the authors

Length: L_x	148mm	5.8 in
Width: L_y	114mm	4.5 in
Thickness: t	6μm	0.25 mils
Young's modulus: E	4.6GPa	650,000 psi
Poisson's ratio: ν	0.3	

Table 2: Nominal Web Specifications

Although it does not enter into "tension field" theory, we list the nominal web thickness for later comparison with "thick" web solutions in the section titled "Cases 7 and 8: Comparison to a Post-Buckled Plate Solution".

It will be noted at the outset that the stress state in this web will be largely uniaxial, with significant tensile stresses forming in the horizontal x direction, and small stress components in the vertical y direction, and in shear. Poisson effects, and variations in the boundary conditions will cause a slight variation on this first-order stress state. Because all elements will be close to the taut/wrinkled transition, small changes in the right edge displacements should reveal significant changes in the wrinkling coverage.

Using this finite element model we have created results for six cases of wrinkling patterns, shown in figure 4-9. At the left of each of these figures is a wrinkling pattern diagram, and to the right is a contour plot for the largest tensile stress.

These stresses have been scaled to the Young's modulus. For each wrinkled element from the FEWA code we have marked a line to show the orientation of a wrinkled element. The length of the wrinkle line is proportional to the magnitude of the tensile stress in the element, and are scaled to the maximum stress in the problem. Elements that are taut are shown without any markings. No appreciable slack regions developed in any of these examples.

Cases 1-3 (Figures 4-6) are given artificial right-edge boundary conditions, chosen to illustrate some basic wrinkling patterns in response to nonuniform loading. Cases 4 and 5 (Figures 7 and 8) utilize boundary conditions that may be expected to arise in transport through a nip. They are drawn from a companion paper in this conference by Diehl, Stack and Benson [23]. Case 6 (Figure 9) is a shear panel example that will be used for comparison to a finite element solution that accounts for out-of plane bending. We will discuss the wrinkling patterns of Cases 1-6 individually, and then make some general observations on the stress contours.

Case 1 depicts a situation where the right edge displacement is greater towards the center than at the edge. This has led to a significant wrinkling coverage in the web. A taut region develops near the back edge due to a Poisson contraction. The greatest stresses occur near the center of the web, and there is a general tendency to develop a "rivers" type wrinkling pattern at the center.

Case 2 contrasts with Case 1 in that the larger edge displacement occurs at the top and bottom, rather than at the middle. Although the resultant loading is the same, the wrinkling coverage is quite different. The web is mostly taut. The Poisson effect, with greater loading near the top and bottom edges leads to a large region that has two tensile principal stresses, albeit the y direction stress will be much less than the x direction stress. A line of wrinkled elements is observed near the top and bottom edges. A "lakes" type wrinkling pattern develops near the center of the right edge.

Case 3 has a nonuniform loading that varies from 2×10^{-3} at the top to 1×10^{-3} at the bottom. This imparts a slight shear on the web, which is revealed by the angle of the wrinkle lines. The greater principal stresses, as expected, form near the top of the web. The unmarked portions of the web are taut.

Case 4 is based on the nip transport results for two hollow cylinders in reference [22]. We have scaled the right-edge displacement according to the normalized speed ratio shown in Figure 10a (shell theory) of reference [22]. As with Figures 4-6, the displacement ranges from 1×10^{-3} to 2×10^{-3} nondimensional units of deflection. The loading will be seen to have a general similarity to Case 2, with the overdrive near the top and bottom sides of the web. The wrinkling pattern that develops is somewhat similar to Case 2. A line of wrinkles forms near the sides, with the beginnings of a "lakes" pattern near the middle. Because of the sharp change in the displacement near the sides there is a large stress concentration near the points of peak displacement.

Case 5 is based on the calendering design results of reference [23], Figure 10b. A soft, thick, rubber-like roller has been pressed onto a rigid roller to form the nip.

Once again the edge displacements have been scaled from $1\text{x}10^{-3}$ to $2\text{x}10^{-3}$ nondimensional units. This displacement pattern shows considerable uniformity, except for a "slow-down" in transport speed due to boundary conditions at the top and bottom edges of the nip. This is due *only* to edge effects in the deformable roller. Figure 8 shows a near-uniform stress and wrinkling pattern through the center of the web. Near the points of right-edge displacement variation, however, large stresses develop, and the web seeks to form very localized "lakes" type wrinkling patterns.

Case 6 is a shear panel result. In addition to a $1\text{x}10^{-3}$ nondimensional rightward stretch, there is also a $2\text{x}10^{-3}$ shearing displacement on the right edge. Taut regions develop at the lower left and upper right corners. The upper left and lower right corners are nearly slack. Wrinkle lines fan out from the lower left and upper right regions, and cover most of the web. Through the middle of the web, the wrinkles align with the diagonally opposite corners that have been pulled further apart (i.e. lower left and upper right). As dictated by free edge boundary conditions, the wrinkle lines follow the web edges near the top and bottom. These are the same approximate conditions that led to the shear wrinkles seen in Figure 2 (bottom).

Stress Contours

On the right side of Figures 4-9 we show maximum tensile stress contours for the six cases just discussed. The average strain on the right edge is roughly $1.5\text{x}10^{-3}$ (a little less for Case 4, and a little more for Case 5), and this leads to a nominal principal stress of about the same value $\sigma_{max}/E = 1.5\text{x}10^{-3}$ towards the center of the web. The stress contours in Figures 4-9 show where the stress concentrations will occur, and where regions of light loading will occur. These stresses correlate with the length of the wrinkle lines shown at the left in Figures 4-9. The entire problems scales linearly in the Young's modulus, E, and the length of the web, L_x. See Table 2.

Cases 7 and 8: Comparison to a Post-Buckled Plate Solution:

To test the FEWA numerical model we have made a comparison (to the extent that is possible) to the results obtained from a post-buckled plate analysis. The system for comparison is the shear panel of Case 6, and the comparison solution is generated by the commercial, nonlinear, finite element code, ABAQUS. We chose ABAQUS because of its ability to compute answers in the post-buckled regime, and because it has been used successfully in other wrinkling analyses. See, for example, the paper by Gopal and Kedl [21], where shear wrinkles were predicted for a web span with an out-of-tram roller.

Our ABAQUS solution was applied to the Case 6 web described above. Results are shown in Figures 10 and 11, as Cases 7 and 8, respectively. Because a full accounting took place of the out-of-plane bending of the web, it was necessary to specify a web thickness for these examples. In Case 7 the thickness is $0.811\text{x}10^{-3}$ times the length of the long edge, and in Case 8 the web thickness ratio is $0.405\text{x}10^{-3}$. In dimensional terms, for a 148mm x 114mm web, we have analyzed two

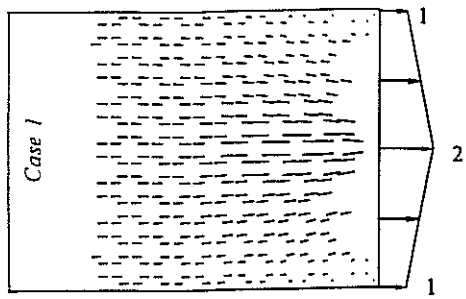

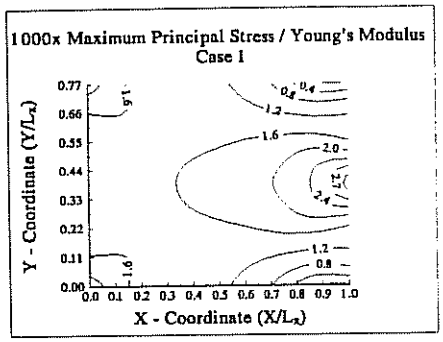

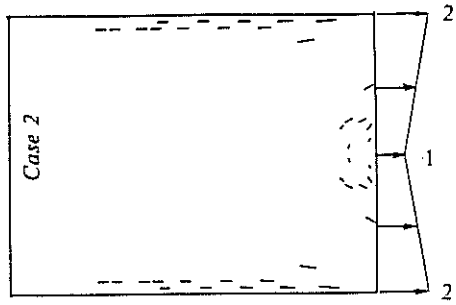

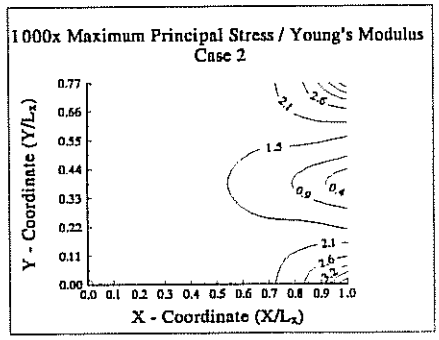

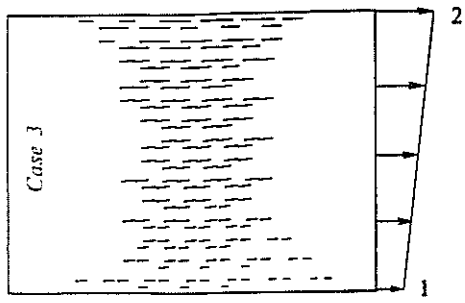

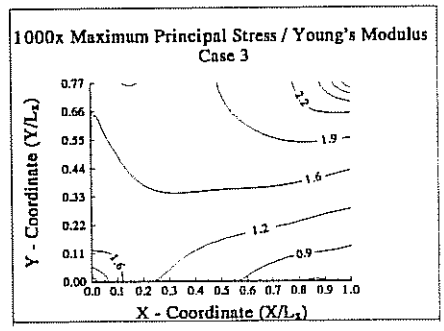

Figures 4-6: Cases 1-3
Wrinkling Patterns (left), Stress Contours (right)

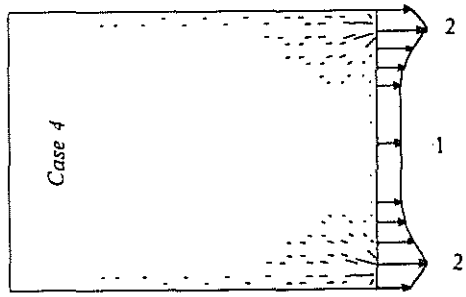

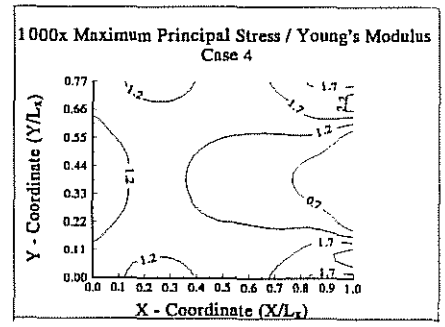

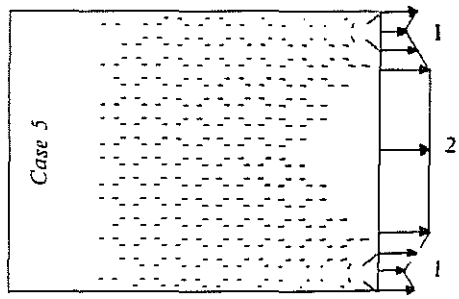

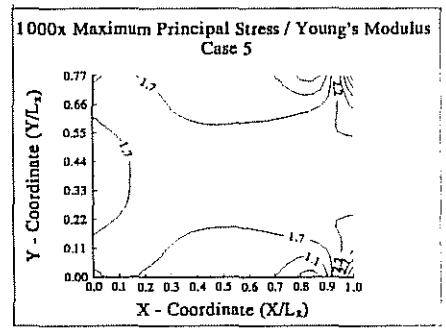

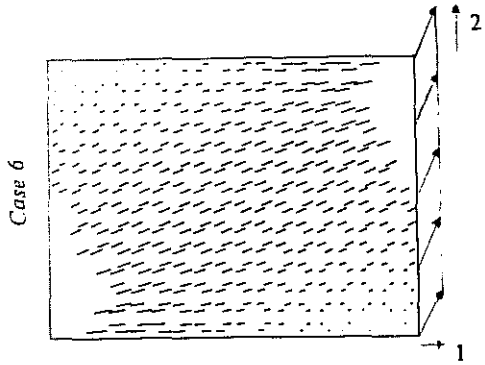

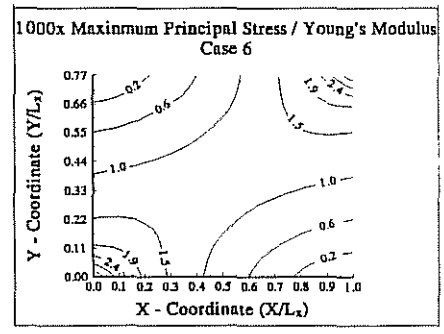

Figures 7-9: Cases 4-6
Wrinkling Patterns (left), Stress Contours (right)

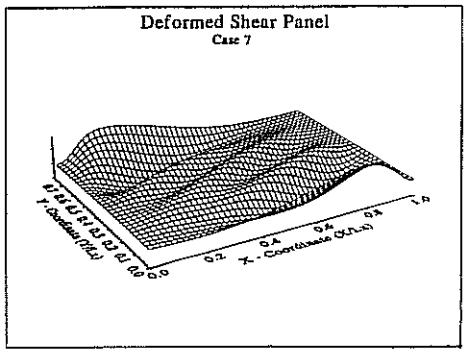

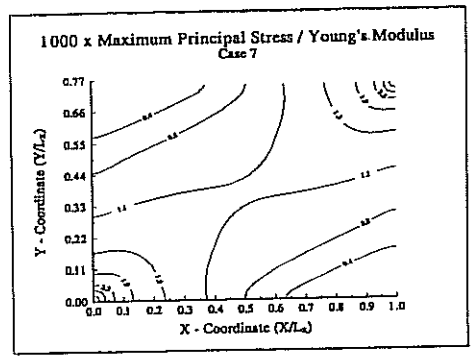

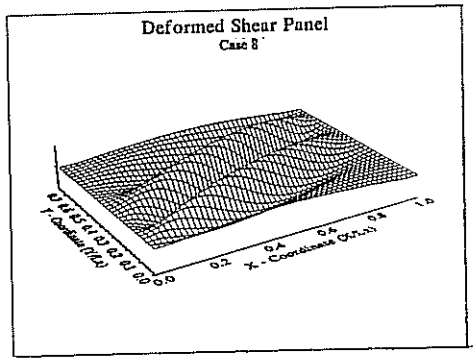

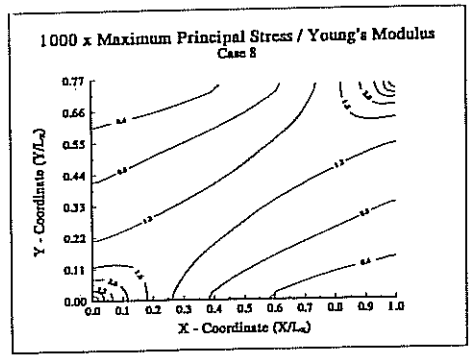

Figures 10-11: Cases 7-8
Buckling Patterns (left), Stress Contours (right)

thicknesses of 120μm and 60μm. These are 20 times, and 10 times the 6μm thickness of the nominal web in Table 2.

The results of Figures 10 and 11 show that the out-of-plane "wrinkling" (it is more of a buckling problem at this thickness) is dominated by the same lower-left to upper-right diagonal seen in Case 6. The wavelength of the wrinkles is quite large. Short wavelengths are resisted by the bending rigidity of the web, which scales with the quantity:

$$D = Et^3/[12(1-\nu^2)]. \quad (5)$$

Note that this is proportional to the thickness, t, cubed. For the dimensional versions of Cases 7 and 8, the bending rigidities are $D = 0.73\text{x}10^{-3}$ Nm and $D = 91\text{x}10^{-6}$ Nm, respectively. These values should be contrasted with the Table 2 specification that motivated Cases 1-6. At 6μm thickness we get $D = 91\text{x}10^{-9}$ Nm.

This is roughly 8,000 and 1,000 times more flexible in bending than the "thick" webs of Cases 7 and 8, and it also provides an answer to the natural question: "Why not perform an ABAQUS solution for thinner webs closer to the 6μm web of interest?" A thickness of 60μm was about as thin as we could make our membrane before numerical difficulties arose in converging on the post-buckled solution using ABAQUS.

The stress contours for maximum midsurface tensile stresses on the right hand sides of Figures 10 and 11 look very much like the "tension field" stress patterns shown in Figure 9. So, despite the fact that the out-of-plane buckling is being handled by a very different approach from the "tension field" theory, the assumptions inherent in "tension field" theory about membrane stresses seem to be quite sound.

DISCUSSION

It is important to consider what these results do and do not mean. Wrinkling patterns of the sort shown in Figures 4-9 do *not* necessarily mean that an actual wrinkle will form on the line shown. (Recall that a line is drawn wherever we have an finite element in the wrinkled state.) All webs have some thickness, and some ability to resist compressive stress before bending. When buckling does occur, bending rigidity will limit the wavelength of the wrinkles - something the "tension field" theory cannot predict.

What these results *do* describe is an important limiting condition that is well beyond the reach of most finite element models. Conventional simulations that account for bending deflection would have to be very densely gridded, and have great numerical accuracy to handle the nonlinear, postbuckled, near-singular conditions represented here. For the present paper, our ability to make post-buckled plate calculations deteriorated at about an order of magnitude greater than the desired web thickness (60μm versus 6μm). By sacrificing the ability to predict wrinkling wavelengths, a "tension field" analysis may be employed with a manageable number of nodes and modest numerical accuracy to give useful design information on such questions as: "Where will the stresses be compressive?"; and "If the compression is relieved through buckling, where will the wrinkles form?"

Cases 1 and 2 in Figures 4 and 5 provide an example of the design assessment that may follow from a tension field analysis. The stress contours in both are nearly the same. Case 1, however, shows more of a tendency to wrinkle, albeit this is due to a *very* slight shift of $\sigma_y < 0$ (before wrinkling) in Case 1 to $\sigma_y > 0$ in Case 2. For relatively thick webs, in actual practice, it would probably be the case that neither web would wrinkle. Nevertheless, it would seem that a slight bit of extra-tensioning on the top and bottom sides of the web is more beneficial than extra-tensioning at the middle. It may be possible to adjust nip conditions and other transport mechanisms to achieve this. This would help bias conditions away from wrinkling, and impart a slight cross-tensioning in the web. In fact, considerable nonuniformity can sometimes be used as a design advantage. See, for example the study on conic rollers by Stack and Benson [24]

A study of Cases 4 and 5 in Figures 6 and 7 reveals a not-too-surprising result that flexible webs do not like high loading gradients. What is important to note, here, is that the loading variations that generated these results are due to boundary effects in the nip. In other words, the roller geometries and materials were perfectly uniform *before* loading. Nonuniformity arose due to elastic deformation *after* the rollers were loaded against each other. This suggests that special care has to be taken in evaluating the deformed nip, and that it may be important to contour rollers, or modify material properties so that more uniform loading conditions are produced.

ACKNOWLEDGEMENT

Funding received from the Eastman Kodak Company in support of the Mechanics of Flexible Structures Project is gratefully acknowledged. Thanks are also extended to Mark Fiscella who supplied the fixture for our wrinkled web tests, Ted Diehl who helped make the numerical calculations, and to Ron Pratt who helped make the photographs of Figure 2.

REFERENCES

1. Wagner, H., *Zeitschrift Flugtechne, Motor.*, **20**, p. 533-538, 1929
2. Reissner, E., "On Tension Field Theory", *Proc. 5th Int. Congress of Applied Mechanics*, p. 88-92, 1938.
3. Kondo, K., Iai, T., Moriguti, S., Murasaki, T., "Tension Field Theory", *Memoirs of the Unifying Study of the Basic Problems in Engineering Science by Means of Geometry*, **I**, p. 417-441, 1955.
4. Mansfield, E.H., "Tension Field Theory", *Proc. XII Int. Congress of Applied Mechanics*, p. 305-329, 1968.
5. Mansfield, E.H., "Load Transfer via a Wrinkled Membrane", *Proc. Royal Society of London A*, **316**, p. 269-289, 1970.
6. Mansfield, E.H., "Analysis of Wrinkled Membranes with Anisotropic and Nonlinear Elastic Properties", *Proc. Royal Society of London A*, **353**, p. 475-498, 1977.
7. Wu, C.H., "Nonlinear Wrinkling of Nonlinear Membranes of Revolution", *ASME J. Applied Mechanics*, **45**, p. 533-538, 1978.

8.Wu, C.H., "Large Finite Strain Membrane Problems", *Q. Applied Mathematics*, p. 347-359, 1979.
9. Zak, M., "Dynamics of Films", *J. Elasticity*, **9**, p. 171-175, 1979.
10. Wu, C.H., and Canfield, T.R., "Wrinkling in Finite Plane-Stress Theory", *Q. Applied Mathematics*, p. 179-199, 1981.
11. Zak, M., "Statics of Wrinkling Films", *J. Elasticity*, **12**, p. 51-63, 1982.
12. Miller, R.K., and Hedgepeth, J.M., "An Algorithm of Finite Element Analysis of Partly Wrinkled Membranes", *AIAA J.*, **20**, p. 1761-1763, 1982.
13. Miller, R.K., and Hedgepeth, J.M., "Finite Element Analysis of Partly Wrinkled Membranes", *Computers and Structures*, **20**, p. 631-634, 1985.
14. Darmon, P., and Benson, "Large Inextensional Deformation of Orthotropic Cantilevered Plates With Distributed Loads", *ASME J. Applied Mechanics*, **52**, p. 385-388, 1985.
15. Darmon, P., and Benson, R.C., "Numerical Solution to an Inextensible Plate Theory With Experimental Results", *ASME J. Applied Mechanics*, **53**, p. 886-890, 1986.
16. Pipkin, A.C., "The Relaxed Energy Density for Isotropic Elastic Membranes", *Arch. Rational Mech. Anal.*, **95**, p. 93-115, 1986.
17. Roddemann, D.G., Oomens, C.W., Janssen, J.D., and Drukker, J., "The Wrinkling of Thin Membranes: Part I - Theory", *J. Applied Mechanics*, **54**, p. 884-887, 1987.
18. Roddemann, D.G., Oomens, C.W., Janssen, J.D., and Drukker, J., "The Wrinkling of Thin Membranes: Part II - Numerical Analysis", *J. Applied Mechanics*, **54**, p. 888-892, 1987.
19. Steigmann, D.J., and Pipkin, A.C., "Wrinkling of Pressurized Membranes. *J. Applied Mechanics*, **56**, p. 624-628, 1989.
20. Steigmann, D.J., and Pipkin, A.C., "Axisymmetric Tension Fields", *ZAMP*, **40**, p. 526-542, 1989.
21. Gopal, H., and Kedl, D.M., "Using Finite Element Model to Define How Wrinkles Form in a Single Web Span Without Moment Transfer", *Proceedings of the First International Conference on Web Handling*, Web Handling Research Center, Oklahoma State University, paper no. 21, June 1991.
22. Chiu, H.C., Benson, R.C., Fiscella, M.D., and Burns, S.J., "Mechanical and Thermal Wrinkling of Polymer Membranes", *ASME J. Applied Mechanics*, in press. (Note: a conference paper on the same topic paper appears in the *Proceedings of the 1992 ASME Web Handling Symposium*, ASME Book Number AMD-Vol. 149).
23. Diehl, T., Stack, K.D., and Benson, R.C., "A Study of Three-Dimensional Nonlinear Nip Mechanics", *Proceedings of the Second International Conference on Web Handling*, Web Handling Research Center, Oklahoma State University, June 1993.
24. Stack, K.D., and Benson, R.C., "The Effects of Axial Variation in Nip Mechanics", *Proceedings of the Second International Conference on Advanced Mechatronics"*, Meiji University, Tokyo, Japan, August 1993.

QUESTIONS AND ANSWERS

Q. Why did you use plate elements in the ABAQUS solutions, but triangular elements in the tension field theory solutions?

A. Excellent question. In the ABAQUS solutions, we're able to use a plate type theory, because, again, it's a little bit thicker web. So, for those solutions, I used plate solutions, which were quadratic. Now again, no one likes to use triangular elements, because they're constant pressure elements, but for the case of wrinkling, we have no choice. That's the only theory that's out there. So, again, for the ABAQUS solutions, that's a normal nonlinear finite element technique.

Q. In web handling, we call what you predicted troughs? Any comments?

A. Yes, that's a good point. In media handling, it's the opposite. So, again, we're not used to the web handling terminology.

Q. Do you ever get wrinkles in the nip?

A. When you say inside the nip?

Q. Actual folding of the web itself inside the nip?

A. Yes, it will. What we use this mostly for is to determine, when we're doing imaging, whether or not we'll be able to image. Because if we have any wrinkles at all, or rather wrinkles in the area that being imaged, we've had it, you know, the copy comes out completely destroyed. As far as the web actually going into the nip, one of the things that we are working on right now is sort of solving a couple of problems. We're actually modelling the web and the nip together and that's really where all of this stuff is leading.